

Article

# Assessment of a Smart Sensing Shoe for Gait Phase Detection in Level Walking

Nicola Carbonaro <sup>1</sup>, Federico Lorussi <sup>1</sup> and Alessandro Tognetti <sup>1,2,\*</sup>

<sup>1</sup> Research Center “E. Piaggio”, University of Pisa, Largo Lucio Lazzarino 1, 56126 Pisa, Italy; nicola.carbonaro@centropiaggio.unipi.it (N.C.); f.lorussi@ing.unipi.it (F.L.)

<sup>2</sup> Information Engineering Department, University of Pisa, via G. Caruso 16, 56122 Pisa, Italy

\* Correspondence: a.tognetti@centropiaggio.unipi.it

Academic Editor: Enzo Pasquale Scilingo; Mostafa Bassiouni

Received: 15 August 2016; Accepted: 4 November 2016; Published: 16 November 2016

**Abstract:** Gait analysis and more specifically ambulatory monitoring of temporal and spatial gait parameters may open relevant fields of applications in activity tracking, sports and also in the assessment and treatment of specific diseases. Wearable technology can boost this scenario by spreading the adoption of monitoring systems to a wide set of healthy users or patients. In this context, we assessed a recently developed commercial smart shoe—the *FootMoov*—for automatic gait phase detection in level walking. FootMoov has built-in force sensors and a triaxial accelerometer and is able to transmit the sensor data to the smartphone through a wireless connection. We developed a dedicated gait phase detection algorithm relying both on force and inertial information. We tested the smart shoe on ten healthy subjects in free level walking conditions and in a laboratory setting in comparison with an optical motion capture system. Results confirmed a reliable detection of the gait phases. The maximum error committed, on the order of 44.7 ms, is comparable with previous studies. Our results confirmed the possibility to exploit consumer wearable devices to extract relevant parameters to improve the subject health or to better manage his/her progressions.

**Keywords:** wearable technology; gait phase; gait cycle, accelerometers; force sensors; walking; smart shoe

---

## 1. Introduction

In the last decade, many groups have carried out research and development on wearable electronics and sensors for unobtrusive, ambulatory and daily-life monitoring of human subjects. The results obtained have shown the possibility to use personal wearable devices to assist and support chronic patients [1–7], elderly people [8,9], emergency operators [10,11] and also healthy subjects for sports, wellness and prevention [12–14]. At the same time, the wearable technology market has exploded and is expected to further increase over the next few years, as proved by the growing interest of big players such as Google, Apple and Samsung.

The current trend is to augment objects worn on the body—e.g., watches, glasses, bracelets—with information and communications technology (ICT) to enable a bi-directional data exchange with a smartphone. These wearable devices or simply *wearables* have been initially conceived as technological *gadgets* but have the potential to support the user in the self-management of his/her health and wellness. Indeed, smart bracelets and/or watches can include physiological (e.g., photoplethysmography, electrodermal activity) or inertial (accelerometers, gyroscopes) sensors able to perform real-time monitoring of subject’s health parameters and movement/physical activity. Recent studies have reported the first attempts to employ smart watches/bracelets in e-health applications [15–19] and many more are expected in the years to come.

Another trend, less explored but not less promising, is to embed ICT devices inside the shoe. The shoe is the ideal place to integrate sensors and communications technology: it has enough space for the micro-devices and it is the object that every one wears for most of the day. This last aspect is the key factor to enable user's acceptance, as the user does not have to wear additional items and the technology can be completely *hidden* and *transparent* for him/her. The integration of inertial and force sensors in the shoe may enable a wide number of applications, ranging from simple activity/fitness tracking (e.g., activity classification, step count, burned calories) fragile people assistance (e.g., fall detection, pedestrian navigation) to complex biomedical assessment and gait analysis.

*Gait analysis* is the study of human locomotion, and it is used to assess and treat patients with conditions affecting their walking activity [20]. The way we walk consists of consecutive *gait cycles*. Each gait cycle includes a predefined sequence of phases (Heel-strike HS, Stance ST, Heel-off HO, Swing SW; see Appendix A for a reference on the adopted terminology). Both *temporal* and *spatial* gait parameters are important to assess a disease and/or a traumatic event, and also to define and optimize the treatment (e.g., rehabilitation, physical therapy). The temporal and spatial gait parameters are used in many biomedical and e-health applications, such as assessment of the recovery in stroke patients [21,22] and gait-cycle-based control of functional electrical stimulators (FES) for *drop foot* compensation [23–25]. In the robotic rehabilitation field, the quantitative evaluation of the gait parameters allows the quantification of the improvements of the gait patterns [26]. In addition, the spatial gait parameters, such as stride length, can be associated with fall risk [27], or elaborated for foot motion localization in applications such as emergency operator rescue and pedestrian navigation [28–31].

The reviews from Rueterbories et al. [32] and from Taborri et al. [33] provide a full overview of the gait phase detection methods and technologies. Many research works performed gait phase detection through inertial sensors (accelerometers, gyroscopes, inertial measurement units - IMU) applied to different body segments (pelvis, thigh, shank, foot) [34–38]. As a recent relevant example, the work of Van Nguyen et al. [39] focuses on an IMU sensor for an accurate estimation of foot position, velocity and attitude. Many other works were focused on *on-foot* sensors. Most of the *on-foot* systems dealt with force based methods, employing foot-switches or force sensitive resistors (FSRs) to measure the body/ground force interaction [40–42]. Force based methods have reliable performance, but are unable to discriminate walking activities from load changes (i.e., in foot drop control, this implies the user turning off the detection/control system at the end of the walking activity). To solve this issue, Pappas et al. [43] combined force and inertial sensors to obtain a reliable gait phase detection system, able to discriminate walking activities from load shifting in static tasks. They employed three FSRs (one under the heel and two under the fore-foot region) and a gyroscope attached to the back side of the shoe (above the heel). Force sensors detected the foot loading/unloading, while the gyroscope estimated the foot inclination and rotational velocity. In their work, Pappas et al. [43] detected four gait phases through a state machine whose transitions were governed by a rule based algorithm applying predefined thresholds on the parameters extracted from the sensors (foot loading/unloading, inclination, rotational velocity). Other examples of force and inertial sensors combination can be found in [44,45]. As underlined in [33], gait phase partitioning algorithms can be divided into three main classes. *Threshold-based* methods—such as the above reported from Pappas et al. [43]—which apply predefined or adaptive thresholds to the sensor signals, are simple and are often suitable for integration in embedded systems. *Machine learning* methods and in particular Hidden Markov Models (HMM) are more complex than threshold based methods but have shown improved performance in gait phase detection. As a relevant example, Mannini and Sabatini [37] developed an HMM classifier which detected four gait phases from an uni-axial foot-mounted gyroscope, and achieved significantly better performance than the threshold-based method applied to the same dataset. A more recent trend is to apply hierarchical decision to the output of two or more HMMs. As reported in the work from Taborri et al. [38], *hierarchical* methods provide excellent performance and are compatible with real-time implementation.

In-shoe sensor systems have been commonly developed for real-time detection of gait parameters and walking patterns with applications in the assessment of specific foot pathologies (e.g., flat foot [46], diabetic foot [47]) and posture/activity recognition for healthy subjects [48–50] or people affected by neurological conditions such as stroke [51,52] or cerebral palsy [26,53]. In-shoe sensor systems are generally based on movable pressure sensing insoles and/or inertial sensors, combined with an external electronic module (signal acquisition/pre-elaboration, data transmission). Examples of in-shoe systems can be found in the works from Edgar et al. [41] and Bae et al. [54].

Commercial products are limited to professional instruments for clinical evaluation and to a few consumer devices for sports and training of healthy users. Professional products include the F-scan [55] (Tekscan Inc., Boston, MA, USA) and the Pedar [56] (Novel Inc., Munich, Germany) systems that are sensing insoles for the monitoring of dynamic temporal and spatial pressure distributions. Example applications of professional products are gait stability analysis [57], gait phase detection [58] and analysis of the gait characteristics during running [59]. Despite the reliable performance and the high spatial resolution, the professional systems are not suitable for long-term monitoring in daily life conditions: both systems are expensive (on the order of several kEuros) and use electrical wires to connect the insole to the waist-worn acquisition system. The consumer products are generally made by applying an external measurement and transmission unit to a dedicated shoe (e.g., *Adidas miCoach*, *Nike + iPod*). The common aspect is the reduced number of sensors (typically only one inertial sensor) and the interaction with the smartphone in which a dedicated app can deliver special information to the users (e.g., workout time, velocity, distance travelled, calories), engaging them for reaching higher performance during physical activity.

In the current paper, we assessed a recently developed commercial smart shoe for automatic gait phase detection in level walking. The prototype we employed is the *FootMoov* smart shoe [60] produced by the Italian shoe factory Carlos srl (Fucecchio, Firenze, Italy). *FootMoov* was originally designed as a mobile game controller and for simple physical activity training and coaching. *FootMoov* can be interfaced with the smartphone through a WiFi connection and has built-in force sensors (heel and forefoot), triaxial accelerometer (forefoot), chargeable battery and acquisition/transmission module. We chose to assess and develop the gait phase detection algorithm for *FootMoov* since, unlike the current professional and consumer products, all of the hardware—including sensors and electronics—is integrated *inside* the shoe, and no external modules or application of additional parts are needed.

On the other side, *FootMoov* is a *consumer* product. Thus the sensor number and locations are not optimized for gait analysis. In addition, the precise sensor locations and orientation inside the shoe is unknown. In accordance with the current trends in wearable technology, the aim of this work is to show the possibility to employ a low cost smart shoe as a tool for biomedical and e-health applications, allowing the continuous and long-term monitoring of users/patients in daily life. To the best of our knowledge, the assessment of such a wearable product does not exist in the current literature.

In particular, we assessed the smart shoe for the real-time quantification of the temporal parameters of gait. We developed a dedicated gait phase detection algorithm that combines the information extracted from the force and accelerometer sensors of the *FootMoov* smart shoe. In a first experiment, we collected data on ten healthy subjects in free level walking conditions to perform a preliminary and qualitative assessment of the system and algorithm performance. In this test, the algorithm recognized 5925 strides over the total amount of 6000 strides (98.7%). In a second test, we performed a quantitative evaluation of the system in comparison with a reference gait phase signal obtained by an optical motion capture instrument. We evaluated the time difference in the onset of the detected gait phases with respect to the reference (mean error of 44.7 ms) and the error in the estimation of the single phase durations (minimum error of 0.036 s for Heel Strike, with a maximum error of 0.11 s for Heel Off).

## 2. Material and Methods

### 2.1. FootMoov

FootMoov is an innovative smart shoe with sensors and an electronic unit fully integrated inside the footwear, below the insole. The wireless (WiFi) connection enables the use of dedicated smartphone or tablet apps for the acquisition and elaboration of the sensor data.

The smart shoe includes two force sensors and one triaxial accelerometer. As shown in Figure 1, the force sensors are located approximately in the center of the heel and forefoot regions, while the accelerometer is positioned below the insole in correspondence of the shoe tip. FootMoov has a built-in battery, chargeable through a mini-USB connector placed in the rear part of the shoe, below the turn on/off switch. Sensors and electronics are integrated in the right shoe only. Inclination and foot movement could be estimated from accelerometer data, while the foot mechanical interaction with the ground can be extracted from the force sensors.



**Figure 1.** The FootMoov prototype. The green arrows indicate the location of the heel and forefoot force sensors (output  $F_h$  and  $F_f$  respectively). The local reference frame of the calibrated accelerometer (outputs  $a_x$ ,  $a_y$ ,  $a_z$ ) is reported in red ( $x_a$ ,  $y_a$ ,  $z_a$ ). In the rear part of the shoe it is possible to see the on/off switch and the mini-USB connector for battery charging.

The accelerometer integrated in the FootMoov system is a tri-axial digital sensor with low power consumption, ultra-compact dimension and 12-bit resolution for a dynamic full scale range of  $\pm 2$  g. Force sensors are analogue force sensitive resistors (FSRs) in which a variation of the electrical resistance is generated when a pressure in the sensing area is applied. The output characteristic of the FSRs is inversely proportional to force. When the sensor is unloaded the resistance is higher than  $2 \text{ M}\Omega$ . Then, when applied load increases, the electrical resistance decreases. An inverting analog circuit amplifies the FSR output before it is digitally converted. The core of the FootMoov electronics is a low-power and low-cost microcontroller. This device manages sensor data acquisition and wireless transmission. In particular, the microcontroller provides the analog-to-digital conversion of force sensors signal and the digital I/O ports for the acquisition of the digital accelerometer data. A WiFi module is integrated in the FootMoov hardware for the transmission of the sensor data packet to remote devices such as smartphones, tablets or PCs. The transmitted packet is composed of the timestamp (microcontroller internal time reference), the accelerometer data (expressed in logical values) and by two more values related to the front and rear force sensor, respectively (logical values corresponding to the converted force signals). By knowing the packet structure and its transmission protocol (i.e., information supplied by the FootMoov producer), we developed a dedicated app to allow the wireless connection and data exchange with FootMoov. This app is able to retrieve, store and visualize in real-time the sensor signals.

The app is based on the TCP/IP protocol in which the FootMoov shoes act as the server while the mobile devices (smartphones, tablets or PCs) are the clients. The client (user) sends a query to the server (FootMoov system) and once the server answers through the client IP address, the connection is established. Then, a “Start” button turns on, and the user can launch the data acquisition session. FootMoov samples and streams the logical values of the converted sensors data to the smartphone (25 Hz).

## 2.2. Gait Phase Detection

To develop our gait phase detection algorithm, we started from a revision of the existing methods. Since FootMoov is endowed with force and inertial sensors (see Section 2.1), we were inspired to create our gait detection algorithm from the one of Pappas et al. [43]. In particular, we employed a similar state machine with four states corresponding to the four gait phases described in Section 1. As described in Section 2.2.1, we pre-processed the FootMoov sensor data to obtain the quantities for the rule based transitions between the machine states. More specifically, we calibrated and processed the triaxial accelerometer signal to extract the foot inclination (the yaw angle  $\psi$ ) and the inclination velocity (the yaw time derivative  $\psi'$ ), and we acquired the heel and fore-foot loading signals from the FootMoov force sensors ( $F_h$  and  $F_f$  respectively). Finally, Section 2.2.2 describes the gait phase detection algorithm applied to pre-processed FootMoov signals.

### 2.2.1. Signal Pre-Processing

We pre-processed the accelerometer signal to estimate the foot inclination (yaw angle  $\psi$ ), required by the phase detection algorithm described in Section 2.2.2. We converted the raw accelerometer signals from logical values to the measured acceleration expressed in units of g. Note that the orientation of the accelerometer inside the shoe is unknown and not necessarily aligned with the reference frame reported in Figure 1 (i.e., due to internal shoe conformation and/or fabrication tolerance). This aspect implies an offset in the detected inclination (i.e., the inclination is not zero when the shoe lies on an horizontal plane). To avoid the inclination offset, we conceived a dedicated calibration phase. The accelerometer calibration is a two-step procedure derived from the one described in our previous work [61]. In the first step, we measured the accelerometer output when the user was standing upright in a natural position to align the z-axis of the accelerometer with the axis  $Z_a$  (in the upright position,  $Z_a$  is supposed parallel to the absolute vertical, see Figure 1). In a second step, starting from the same up-right position, asked the subject to perform a simple foot movement (three consecutive dorsi-flexions of the ankle). This second measurement allows us to obtain the final alignment by applying the transformation (rotation along  $Z_a$ ) that minimizes the variation of the accelerometer x component. Triaxial accelerometers measure both inertial acceleration and local gravity. In static conditions, only the gravity is present and the inclination of the accelerometer with respect to the vertical is known. In these conditions, the Euler angle  $\psi$  (ZYX convention [62]) can be obtained in terms of the accelerometer components:

$$\psi = \text{atan2}(a_y, a_z), \quad (1)$$

where  $\text{atan2}$  is the four quadrant inverse tangent and  $a_x$ ,  $a_y$ , and  $a_z$  are the calibrated accelerometer components expressed in units of g. In dynamic conditions, the estimation of  $\psi$  by the accelerometer components (Equation (1)) is not reliable due to the effect of the inertial acceleration. It is well known that the inclination estimation error increases as the activity intensity increases (e.g., running, jumping). In literature, to overcome this issue, low pass filtering with very low cut-off frequencies [63] or complex Kalman filter based techniques [64] were applied. These techniques can introduce delays that are not compatible with gait phase detection. Considering the accelerometer inside the FootMoov prototype (Figure 1), the yaw angle represents the rotation angle of the foot around the accelerometer x-axis (positive for anti-clockwise rotations). In our application, we can suppose having quasi-static

conditions when the foot is in contact with the ground (from the Heel-strike to the end of the Heel-off phase) and dynamic conditions when the foot is flying forward (Swing phase). As we will describe in Section 2.2.2, our gait phase detection algorithm exploits the inclination information to detect the transitions between Heel-strike to Stance and Stance to Heel-off. In these situations, we can consider the accelerometer in quasi-static conditions and directly apply Equation (1) to the calibrated accelerometer components to obtain the yaw angle ( $\psi$ ).

For the force sensors, we simply scaled the outputs (logical values) to obtain the  $F_h$  and  $F_f$  signals with the following characteristics: (i)  $F_h = 0$  and  $F_f = 0$  when the sensors are unloaded and (ii)  $F_h \approx 1$  and  $F_f \approx 1$  when the sensors are fully loaded. We determined the scale factor after a preliminary experimental session in our laboratory. We recorded data from three subjects requested to walk for 60 s. In this preliminary walking trial, we evaluated the scale factors as the mean of the relative maximum of the force signals ( $S_{F_h} = 1405$  and  $S_{F_f} = 2003$  for the heel and front sensors, respectively). We also evaluated the baselines of  $F_h$  and  $F_f$  as the sum of the mean and the standard deviation of the un-loaded sensors ( $b_{F_h} = 0.008$  and  $b_{F_f} = 0.005$  for the heel and front sensors, respectively).

### 2.2.2. Detection Algorithm

The state machine is reported in Figure 2. Four state transitions ( $E_i, i = 1, \dots, 4$ ) are allowed and correspond to the gait events of the normal walking.

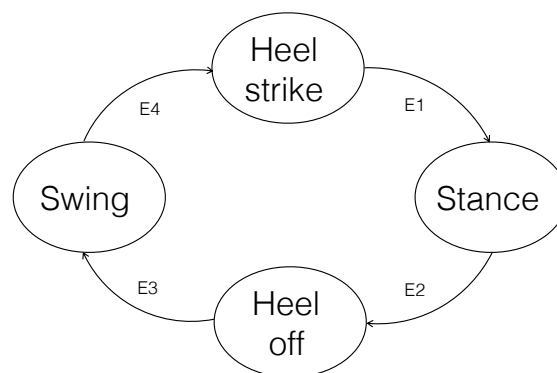


Figure 2. Gait phase detection algorithm.

The state transitions are governed by the following rules:

- E1 (Heel-strike to Stance): in the Heel-strike state, Stance is detected when both heel and fore-foot sensors are loaded or the foot rotational velocity is close to zero ( $[F_h > th_{F_h} \text{ AND } F_f > th_{F_f}] \text{ OR } |\psi'| < \delta_{\psi'}$ );
- E2 (Stance to Heel-off): in the Stance state, Heel-off is detected if the heel sensor is unloaded and the foot inclination angle ( $\psi$ ) exceeds a certain threshold ( $F_h < th_{F_h} \text{ AND } \psi > th_{\psi}$ );
- E3 (Heel-off to Swing): in the Heel-off state, Swing is recognized if heel and fore-foot are unloaded and the rotational velocity turns from positive to negative ( $[F_h < th_{F_h} \text{ AND } F_f < th_{F_f}] \text{ AND } \psi' < 0$ );
- E4 (Swing to Heel-strike): in the Swing state, Heel-strike is detected as the heel touches the ground and the heel sensor is loaded ( $F_h > th_{F_h}$ ).

We also evaluated the stride period as the temporal distance between the onset of two consecutive Heel-strike phases and, accordingly, the cadence as the number of strides per minute. The state machine has the same working frequency of the FootMoov sampling rate (25 Hz).

We set the thresholds of the force sensors as two times their baselines (see Section 2.2.1). We fixed  $th_{\psi} = 0.035$  rad and  $\delta_{\psi'} = 0.52$  rad/s in accordance with the literature values from [43,65]. The 60 s preliminary walking trial was also useful to verify these parameters.

### 2.3. Experiments

To assess the FootMoov system and the gait phase detection algorithm, we conceived two different experimental tests.

#### 2.3.1. Free Walking Experiment

The first test aimed at a qualitative assessment of the prototype and the gait detection algorithm in daily life level walking conditions. Ten healthy subjects were recruited and were asked to walk on level ground. The subjects walked in outdoor conditions in an open space free of obstacles. The subjects had no physical or neurological impairments that affect the characteristics of their walking activity. The subject characteristics were different for age, weight and height, and are reported in Table 1. They were instructed to choose the cadence of a normal walking activity. We requested the subjects to wear the FootMoov shoes and to execute a fixed number of strides (150 strides) repeated for four times. During each session, number of strides, distance traveled and time elapsed were manually stored as useful information for the evaluation of the system and the algorithm developed. Through the app described in Section 2.1, we collected the FootMoov raw data (force sensors and accelerometer) that were transmitted and stored in the smartphone that was kept in the subject's pocket during the walking trials. Data were elaborated off-line in Matlab by applying the pre-processing algorithms of Section 2.2.1 and the gait phase detection algorithm of Section 2.2.2. Here—to obtain a preliminary qualitative evaluation—we compared the number of strides detected by the algorithm (i.e., as occurrence of two consecutive heel strike phases) with the total number of strides (150 for each trial).

**Table 1.** User characteristics.

Age (Mean $\pm$ Std) [Years]	Weight (Mean $\pm$ Std) [kg]	Height (Mean $\pm$ Std) [m]
26.75 $\pm$ 3.1	76.875 $\pm$ 8.5	1.768 $\pm$ 0.06

#### 2.3.2. Motion Capture Experiment

The second test aimed at a quantitative evaluation of the smart shoe and the detection algorithm. We evaluated the FootMoov prototype and our gait phase detection algorithm in comparison with a reference gait phase signal obtained through an optical motion capture device. We adopted a four camera optical motion capture system (Smart DX100 produced by BTS Bioengineering [66]). Two passive markers were applied to the FootMoov shoe, as shown in Figure 3, in correspondence with the tip and heel area. The absolute position of the markers was acquired by the BTS system with a working frequency of 100 Hz. According to [43], we built the gait phase reference signal by applying a rule based algorithm to the vertical positions of the heel and tip markers. Subjects were asked to wear the FootMoov shoes (with the passive markers on) and to walk within the workspace of the cameras (see Figure 3). At the same time, raw sensor data coming from the FootMoov system were acquired and stored in the smartphone. The space used for this experiment was about 5 meters long and 2 meters wide, and the subjects repeated the session four times. Data were again elaborated off-line (pre-processing: Section 2.2.1, gait phase detection: Section 2.2.2) and were synchronised and compared to the reference gait signal.

To synchronize the two acquisition systems (FootMoov and BTS motion capture), we generated a reference signal to determine the time period in which the trial session occurred. The reference signal is a step waveform signal (TTL value) which is “High” during the acquisition period, and “Low” otherwise. This signal, activated by the smartphone app, is used to manage the BTS system through a specific port devoted to external signal acquisition. In particular, we used this step waveform signal as a trigger for the control of the recording session of the motion capture system. Moreover, to double-check the correct data alignment, the subject was requested to perform a particular foot

movement at the beginning of each session. This movement generates a significant variation in both sensor data and marker signals, easily recognizable as a session starting point.



**Figure 3.** Subject performing the trials within the motion capture (BTS system) workspace. The two markers, attached to the right FootMoov shoe at the tip and heel area, are tracked by the BTS system during the walking activity.

The purpose of this experiment was to test FootMoov and our gait phase detection algorithm in terms of duration of the single gait phases and time delay of their onset. We evaluated the mean and the standard deviation of the durations of each gait phase (HS, ST, HO, SW) and compared the values obtained with the reference phase duration statistics. In addition, we calculated the error ( $e_{ij}$ ) expressed as the phase duration difference between our algorithm ( $FM$ ) and the reference ( $REF$ ):  $e_{ij} = \Delta T_{ij}^{FM} - \Delta T_{ij}^{REF}$ , where  $\Delta T$  is the phase duration and  $i$  indicates the gait phase (HS, ST, HO or SW) of the  $j$ -th step. The mean and the standard deviation of the errors ( $e_{ij}$  sequences) were also evaluated. We performed a statistical analysis on the  $e_{ij}$  sequences to verify, for each phase, the null hypothesis that the error in gait phase duration is a zero mean random variable. In particular, we performed a  $t$ -test on each  $e_{ij}$  sequence. The significance level was fixed at  $\alpha = 0.05$ . For each gait phase, the corresponding  $p$ -value of the different samples have been computed. Calculations were performed by using the function  $t$ -test included in Matlab<sup>®</sup> (Mathworks, Massachusetts, MA, USA).

### 3. Results and Discussion

#### 3.1. Free Walking Experiment

Figure 4 shows a typical output of the gait phase detection algorithm for two subjects performing the evaluation test in the outdoors, and in free walking conditions (first test described in Section 2.3.1). The force and accelerometer signals ( $F_h$ ,  $F_f$ ,  $ax$ ,  $ay$ ,  $az$ ) and the detected gait phase signal are reported. The gait phase signal has four levels corresponding to the four gait phases: (1) Heel-strike; (2) Stance; (3) Heel-off; and (4) Swing. We evaluated the number of strides recognised in comparison with the effective number of strides (150 strides, performed by 10 users for four times each, for a total of 6000 steps registered). The algorithm recognized 5925 strides over the total amount of 6000 strides (98.7%). In all the detected steps, we observed the correct sequence of the four gait phases. Despite this being a preliminary and qualitative evaluation (i.e., no comparison with a reference system), it is important to underline that a reliable stride count may be important to estimate the distance travelled, as demonstrated by the study of Truong et al. [67]. Note that, even if we performed an off-line processing, our algorithm can be suitable for real-time implementation (i.e., mandatory for applications such as the drop foot control). To this aim, we estimated the computational load as



the mean time spent by the algorithm (both pre-processing and gait phase detection) to estimate the current state. The value obtained was 0.9 ms and is compatible with real-time implementation.

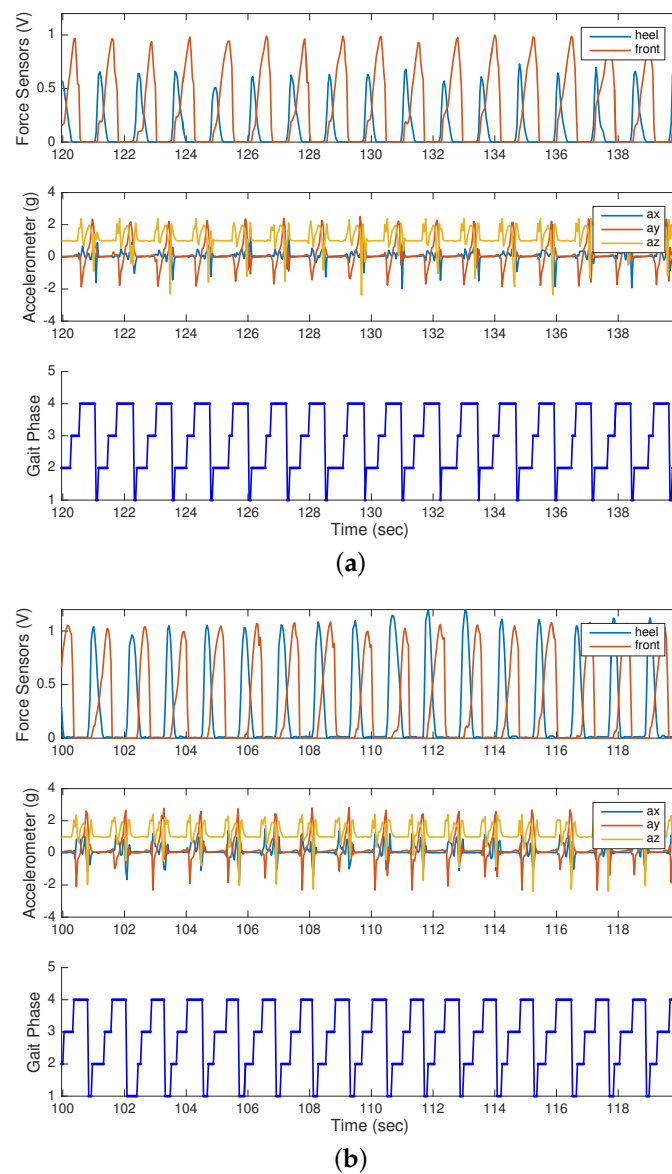


**Figure 4.** Typical output of the gait phase detection algorithm for two different subjects. Each subfigure - **(a)** and **(b)** - reports the sensor signal and the gait phase detection for one subject. In the top graphs, the force value  $F_h$  and  $F_f$  are reported. The middle figures report the calibrated accelerometer components ( $a_x$ ,  $a_y$ ,  $a_z$ ). The bottom traces are related to the detected gait phases.

### 3.2. Motion Capture Experiment

Figure 5 shows a typical comparison between the FootMoov gait phase detection and the reference signal obtained by the optical motion capture system (second test described in Section 2.3.2).

For a first quantitative evaluation, we calculated the average time delay that affected the onset of the gait phase detection. The average delay among the four phases was 44.7 ms. This delay was comparable with the results of previous studies such as [43]. Note that the low sample frequency (25 Hz) of Footmoov introduces a time resolution of 40 ms, comparable with the error committed.

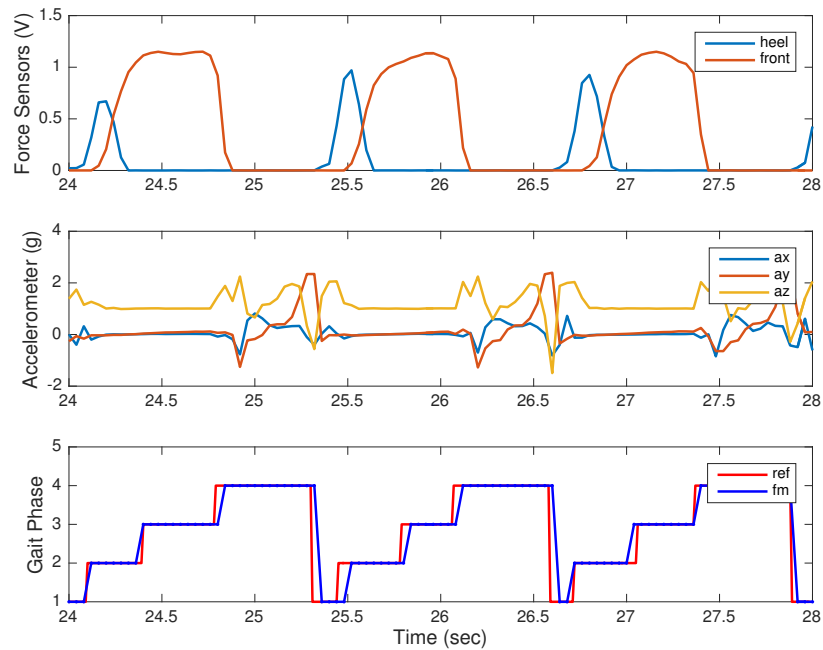


**Figure 5.** Comparison of our gait phase detection algorithm and the reference gait phase signal. In the top graph, the force value  $F_h$  and  $F_f$  are reported. The middle figure reports the calibrated accelerometer components ( $a_x$ ,  $a_y$ ,  $a_z$ ). In the bottom figure, the reference gait phase signal is reported in red while the signal obtained by FootMoov elaborated with our detection algorithm is reported in blue.

In addition, Table 2 summarises the performance of the sensing shoe and our gait detection algorithm in terms of duration of the single gait phases detected (for each phase, we extracted the mean and the standard deviations of REF and FM and the related error as defined in Section 2.3.2). For all the four phases, the  $t$ -test performed on the  $e_{ij}$  sequences indicated that the null hypothesis (i.e., the error sequence distribution has zero mean) cannot be rejected. The corresponding  $p$ -values are reported in Table 2. The mean values of the detected and the reference phase durations are comparable. The minimum error (mean + standard deviation) is in the HS phase (0.036 s) while the maximum is in the HO phase (0.11 s). These errors, always lower than 3 times the time resolution, may be due to the fixed system of thresholds (defined in Section 2.2.2) that could not be tailored to the specific characteristics of all the subjects.

**Table 2.** Mean and standard deviation of the duration of the gait phases (REF and FM), mean and standard deviation of errors ( $e_{ij}$ ) and  $p$ -values of the statistical evaluation.

		Mean [s]	Std [s]	$p$
HS	REF	0.125	0.013	
	FM	0.117	0.03	
	e	0.008	0.028	0.3
ST	REF	0.350	0.057	
	FM	0.310	0.098	
	e	0.039	0.065	0.07
HO	REF	0.293	0.061	
	FM	0.249	0.099	
	e	0.044	0.07	0.12
SW	REF	0.535	0.043	
	FM	0.514	0.036	
	e	0.021	0.050	0.25

### 3.3. Study Limitations

Despite the promising performance, several limitations of our work should be mentioned. First, we tested our algorithm for level walking conditions only, without considering other possible typical situations such as stair ascending/descending or walking on irregular ground (i.e., in stair ascending/descending the first contact after the swing phase is not likely to be on the heel). The second limitation is that we tested the system and the algorithm with healthy subjects with normal walking styles (pathological gaits can have different sensor signatures, difficult to be detected by the algorithm). However, our study was conceived as a preliminary evaluation of the commercial wearable technology and as a test for our algorithms to be used in daily life conditions for biomedical applications, but a more intensive testing phase with different walking conditions would be needed. We expect that both issues could be solved by adding new possible transitions between the machine states. Another possible solution would be to study and develop a system of adaptive thresholds that can be tailored to the particular subject's physical characteristic walking style or pathology. The last limitation is related to the reference signal obtained with the optical system. A validation against a force platform would be more solid and will be considered in future works.

## 4. Conclusions

In this paper, we have reported the assessment of a consumer smart sensing shoe for the detection of gait phases during walking activity. We developed a gait phase detection algorithm that fuses data of inertial and force sensors built-in the FootMoov smart shoe. We tested the prototype and the detection algorithm in free level walking conditions on ten healthy subjects and in a laboratory setting in comparison with an optical motion capture system. The combination of force sensors and accelerometers provided a reliable detection of the gait phases and made it possible to discriminate walking activity from load shifting in static tasks. As a preliminary and qualitative result, the algorithm, tested in free walking conditions, recognised 5925 strides over a total amount of 6000 strides (98.7%). To obtain a quantitative evaluation of the performance of the wearable system and the detection technique, we compared the gait phase signal with a reference signal obtained by an optical motion capture instrument. First of all, we extracted the time difference between our gait phase signal and the reference. We achieved a mean delay of 44.7 ms, comparable to previous study in this field, and mostly limited by the low sampling frequency of the smart shoe (25 Hz). In terms of possible applications, the achieved performance may be compatible with real time FES drop foot compensation (errors below 70 ms are considered sufficiently small [68]). We also assessed the reliability of the temporal duration of the gait phases we detected. The mean durations of the single gait phases are comparable.

In conclusion, we have demonstrated the possibility to use a consumer and low cost wearable device for the estimation of temporal parameters of gait. The demonstrated performance and the characteristics of the prototype—that is a conventional shoe that can be worn without any discomfort for the user—may boost the application of such technology in many fields. For example, it may be possible to monitor or prevent specific gait conditions or to manage and coach the recovery from a physical or neurological pathology. Another possible application may be to use the smart shoe as a feedback device to train healthy subjects or athletes in the optimisation of their walking/running behaviour. Future works will be devoted to extensive tests on a wider number of subjects (both normal and pathological walkers) with different walking conditions. The possibility to develop a system of subject-specific or pathology-specific thresholds will also be considered. We will also study the detection of spatial gait parameters to complete the set of relevant parameters that can be extracted by the wearable system.

**Acknowledgments:** The authors thank Luigi Campigli, head of *FootMoov*, for his kind and competent assistance.

**Author Contributions:** N.C., A.T. performed the data acquisition; N.C., F.L., A.T. reviewed the methods and developed the gait detection algorithm; N.C., A.T. elaborated on the data; N.C., A.T. drafted the manuscript; N.C., F.L., A.T. revised and finalized the manuscript.

**Conflicts of Interest:** The authors declare no conflict of interest.

## Appendix A. Temporal and Spatial Gait Parameters

According to the definition from Pappas et al. [43], the normal gait cycle can be divided in four consecutive periods:

- *Heel-strike*: starts with the initial contact of the heel and ends when the entire foot is on the ground;
- *Stance*: the entire foot is in contact with the ground;
- *Heel-off*: the frontal part of the foot touches the ground while the heel is above the ground;
- *Swing*: the foot is not in contact with the ground and moves forward.

The *gait events* are defined as the transitions from one phase to the next. The *walking cycle* is the period from *heel strike* to *heel strike* of the same foot [69].

The main *temporal* gait parameters are: (i) the *stride period*: the time from two consecutive ground contacts of the same foot; (ii) the *step period*: the time from two consecutive ground contacts of different feet; (iii) the duration of the gait phases (Heel-strike, Stance, Heel-off, Swing), normally expressed in percentages to facilitate the comparison between subjects; and (iv) the *cadence*: the number of strides in a minute. The main *spatial* gait parameters are: (i) the *stride length*: distance between two consecutive ground contacts of the same foot; and (ii) the *step length*: distance between two consecutive ground contacts of the different feet. Note that if the step length and the cadence are known, it is possible to determine the step velocity.

## References

1. Amft, O.; Habetha, J. Smart medical textiles for monitoring patients with heart conditions. In *Smart Textiles for Medicine and Healthcare Materials, Systems and Applications*; Woodhead Publishing Limited: Cambridge, UK, 2007; pp. 275–301.
2. Valenza, G.; Nardelli, M.; Lanata, A.; Gentili, C.; Bertschy, G.; Paradiso, R.; Scilingo, E.P. Wearable monitoring for mood recognition in bipolar disorder based on history-dependent long-term heart rate variability analysis. *IEEE J. Biomed. Health Inform.* **2014**, *18*, 1625–1635.
3. Carbonaro, N.; Anania, G.; Mura, G.; Tesconi, M.; Tognetti, A.; Zupone, G.; de Rossi, D. Wearable biomonitoring system for stress management: A preliminary study on robust ECG signal processing. In *Proceedings of the 2011 IEEE International Symposium on a World of Wireless, Mobile and Multimedia Networks (WoWMoM)*, Lucca, Italy, 20–24 June 2011.
4. Patel, S.; Park, H.; Bonato, P.; Chan, L.; Rodgers, M. A review of wearable sensors and systems with application in rehabilitation. *J. Neuroeng. Rehabil.* **2012**, *9*, 32.
5. Tognetti, A.; Lorussi, F.; Dalle Mura, G.; Carbonaro, N.; Pacelli, M.; Paradiso, R.; de Rossi, D. New generation of wearable goniometers for motion capture systems. *J. Neuroeng. Rehabil.* **2014**, *11*, doi:10.1186/1743-0003-11-56.
6. Dalle Mura, G.; Lorussi, F.; Tognetti, A.; Anania, G.; Carbonaro, N.; Pacelli, M.; Paradiso, R.; de Rossi, D. Piezoresistive goniometer network for sensing gloves. In *Proceedings of the XIII Mediterranean Conference on Medical and Biological Engineering and Computing 2013*, Seville, Spain, 25–28 September 2013; Volume 41, pp. 1547–1550.
7. Carbonaro, N.; Dalle Mura, G.; Lorussi, F.; Paradiso, R.; De Rossi, D.; Tognetti, A. Exploiting wearable goniometer technology for motion sensing gloves. *IEEE J. Biomed. Health Inform.* **2014**, *18*, 1788–1795.
8. Wagner, F.; Basran, J.; Dal Bello-Haas, V. A review of monitoring technology for use with older adults. *J. Geriatr. Phys. Ther.* **2012**, *35*, 28–34.
9. Baig, M.M.; Gholamhosseini, H.; Connolly, M.J. A comprehensive survey of wearable and wireless ECG monitoring systems for older adults. *Med. Biol. Eng. Comput.* **2013**, *51*, 485–495.
10. Bonfiglio, A.; Carbonaro, N.; Chuzel, C.; Curone, D.; Dudnik, G.; Germagnoli, F.; Hatherall, D.; Koller, J.; Lanier, T.; Loriga, G.; et al. Managing catastrophic events by wearable mobile systems. In *Proceedings of the Mobile Response: First International Workshop on Mobile Information Technology for Emergency Response, Mobile Response 2007*, Sankt Augustin, Germany, 22–23 February 2007; Revised Selected Papers; Lecture Notes in Computer Science; Springer: Berlin/Heidelberg, Germany, 2007; pp. 95–105.

11. Klann, M. Tactical Navigation Support for Firefighters: The LifeNet Ad-Hoc Sensor-Network and Wearable System. In Proceedings of the Mobile Response: Second International Workshop on Mobile Information Technology for Emergency Response, MobileResponse 2008, Bonn, Germany, 29–30 May 2008; Revised Selected Papers; Lecture Notes in Computer Science; Springer: Berlin/Heidelberg, Germany, 2009; pp. 41–56.
12. Tesconi, M.; Tognetti, A.; Scilingo, E.; Zupone, G.; Carbonaro, N.; De Rossi, D.; Castellini, E.; Marella, M. Wearable sensorized system for analyzing the lower limb movement during rowing activity. In Proceedings of the IEEE International Symposium on Industrial Electronics 2007, Vigo, Spain, 4–7 June 2007; pp. 2793–2796.
13. Chambers, R.; Gabbett, T.J.; Cole, M.H.; Beard, A. The use of wearable microsensors to quantify sport-specific movements. *Sports Med.* **2015**, *45*, 1065–1081.
14. Redfern, J. The Evolution of Physical Activity and Recommendations for Patients with Coronary Heart Disease. *Heart Lung Circ.* **2016**, *25*, 759–764.
15. Arberet, S.; Lemay, M.; Renevey, P.; Sola, J.; Grossenbacher, O.; Andries, D.; Sartori, C.; Bertschi, M. Photoplethysmography-based ambulatory heartbeat monitoring embedded into a dedicated bracelet. *Comput. Cardiol.* **2013**, *40*, 935–938.
16. Hataji, O.; Kobayashi, T.; Gabazza, E. Smart watch for monitoring physical activity in patients with chronic obstructive pulmonary disease. *Respir. Investig.* **2016**, *54*, 294–295.
17. Wile, D.; Ranawaya, R.; Kiss, Z. Smart watch accelerometry for analysis and diagnosis of tremor. *J. Neurosci. Methods* **2014**, *230*, 1–4.
18. Wijaya, R.; Setijadi, A.; Mengko, T.; Mengko, R. Heart rate data collecting using smart watch. In Proceedings of the 2014 IEEE 4th International Conference on System Engineering and Technology (ICSET 2014), Bandung, Indonesia, 24–25 November 2014.
19. Militara, A.; Frandes, M.; Lungeanu, D. Smart wristbands as inexpensive and reliable non-dedicated solution for self-managing type 2 diabetes. In Proceedings of the 2015 E-Health and Bioengineering Conference (EHB 2015), Iasi, Romania, 19–21 November 2015.
20. Perry, J.; Burnfield, J.M. *Gait Analysis: Normal and Pathological Function*; Slack: Thorofare, NJ, USA, 1992.
21. Lopez-Meyer, P.; Fulk, G.D.; Sazonov, E.S. Automatic detection of temporal gait parameters in poststroke individuals. *IEEE Trans. Inf. Technol. Biomed.* **2011**, *15*, 594–601.
22. Balasubramanian, C.K.; Neptune, R.R.; Kautz, S.A. Variability in spatiotemporal step characteristics and its relationship to walking performance post-stroke. *Gait Posture* **2009**, *29*, 408–414.
23. Kotiadis, D.; Hermens, H.; Veltink, P. Inertial Gait Phase Detection for control of a drop foot stimulator: Inertial sensing for gait phase detection. *Med. Eng. Phys.* **2010**, *32*, 287–297.
24. Blaya, J.A.; Herr, H. Adaptive control of a variable-impedance ankle-foot orthosis to assist drop-foot gait. *IEEE Trans. Neural Syst. Rehabil. Eng.* **2004**, *12*, 24–31.
25. Lyons, G.M.; Sinkjær, T.; Burridge, J.H.; Wilcox, D.J. A review of portable FES-based neural orthoses for the correction of drop foot. *IEEE Trans. Neural Syst. Rehabil. Eng.* **2002**, *10*, 260–279.
26. Meyer-Heim, A.; Ammann-Reiffer, C.; Schmartz, A.; Schaefer, J.; Sennhauser, F.H.; Heinen, F.; Knecht, B.; Dabrowski, E.; Borggraefe, I. Improvement of walking abilities after robotic-assisted locomotion training in children with cerebral palsy. *Arch. Dis. Child.* **2009**, *94*, 615–620.
27. Thaler-Kall, K.; Peters, A.; Thorand, B.; Grill, E.; Autenrieth, C.S.; Horsch, A.; Meisinger, C. Description of spatio-temporal gait parameters in elderly people and their association with history of falls: results of the population-based cross-sectional KORA-Age study. *BMC Geriatr.* **2015**, *15*, 1.
28. Nguyen, L.V.; La, H.M.; Sanchez, J.; Vu, T. A Smart Shoe for building a real-time 3D map. *Autom. Constr.* **2016**, *71*, 2–12.
29. Foxlin, E. Pedestrian tracking with shoe-mounted inertial sensors. *IEEE Comput. Graph. Appl.* **2005**, *25*, 38–46.
30. Jiménez, A.R.; Seco, F.; Prieto, J.C.; Guevara, J. Indoor pedestrian navigation using an INS/EKF framework for yaw drift reduction and a foot-mounted IMU. In Proceedings of the 2010 7th IEEE Workshop on Positioning Navigation and Communication (WPNC), Dresden, Germany, 11–12 March 2010; pp. 135–143.
31. Van Nguyen, L.; La, H.M. A human foot motion localization algorithm using IMU. In Proceedings of the 2016 American Control Conference (ACC), Boston, MA, USA, 6–8 July 2016; pp. 4379–4384.
32. Rueterbories, J.; Spaich, E.G.; Larsen, B.; Andersen, O.K. Methods for gait event detection and analysis in ambulatory systems. *Med. Eng. Phys.* **2010**, *32*, 545–552.

33. Taborri, J.; Palermo, E.; Rossi, S.; Cappa, P. Gait partitioning methods: A systematic review. *Sensors* **2016**, *16*, 66.
34. Mansfield, A.; Lyons, G.M. The use of accelerometry to detect heel contact events for use as a sensor in FES assisted walking. *Med. Eng. Phys.* **2003**, *25*, 879–885.
35. Aminian, K.; Najafi, B.; Büla, C.; Leyvraz, P.F.; Robert, P. Spatio-temporal parameters of gait measured by an ambulatory system using miniature gyroscopes. *J. Biomech.* **2002**, *35*, 689–699.
36. Williamson, R.; Andrews, B.J. Gait event detection for FES using accelerometers and supervised machine learning. *IEEE Trans. Rehabil. Eng.* **2000**, *8*, 312–319.
37. Mannini, A.; Sabatini, A.M. Gait phase detection and discrimination between walking–jogging activities using hidden Markov models applied to foot motion data from a gyroscope. *Gait Posture* **2012**, *36*, 657–661.
38. Taborri, J.; Rossi, S.; Palermo, E.; Patanè, F.; Cappa, P. A novel HMM distributed classifier for the detection of gait phases by means of a wearable inertial sensor network. *Sensors* **2014**, *14*, 16212–16234.
39. Van Nguyen, L.; La, H.M. Real-Time Human Foot Motion Localization Algorithm With Dynamic Speed. *IEEE Trans. Hum.-Mach. Syst.* **2016**.
40. Smith, B.T.; Coiro, D.J.; Finson, R.; Betz, R.R.; McCarthy, J. Evaluation of force-sensing resistors for gait event detection to trigger electrical stimulation to improve walking in the child with cerebral palsy. *IEEE Trans. Neural Syst. Rehabil. Eng.* **2002**, *10*, 22–29.
41. Edgar, S.R.; Swyka, T.; Fulk, G.; Sazonov, E.S. Wearable shoe-based device for rehabilitation of stroke patients. In Proceedings of the 2010 Annual International Conference of the IEEE Engineering in Medicine and Biology, 2010, Buenos Aires, Argentina, 31 August–4 September 2010; pp. 3772–3775.
42. Kong, K.; Tomizuka, M. Smooth and continuous human gait phase detection based on foot pressure patterns. In Proceedings of the IEEE International Conference on Robotics and Automation (ICRA 2008), Pasadena, CA, USA; 19–23 May 2008; pp. 3678–3683.
43. Pappas, I.P.; Popovic, M.R.; Keller, T.; Dietz, V.; Morari, M. A reliable gait phase detection system. *IEEE Trans. Neural Syst. Rehabil. Eng.* **2001**, *9*, 113–125.
44. Senanayake, C.M.; Senanayake, S.A. Computational intelligent gait-phase detection system to identify pathological gait. *IEEE Trans. Inf. Technol. Biomed.* **2010**, *14*, 1173–1179.
45. Hegde, N.; Sazonov, E. SmartStep: A Fully Integrated, Low-Power Insole Monitor. *Electronics* **2014**, *3*, 381–397.
46. Tareco, J.M.; Miller, N.H.; MacWilliams, B.A.; Michelson, J.D. Defining flatfoot. *Foot Ankle Int.* **1999**, *20*, 456–460.
47. Mueller, M.J.; Hastings, M.; Commean, P.K.; Smith, K.E.; Pilgram, T.K.; Robertson, D.; Johnson, J. Forefoot structural predictors of plantar pressures during walking in people with diabetes and peripheral neuropathy. *J. Biomech.* **2003**, *36*, 1009–1017.
48. Sazonov, E.S.; Bumpus, T.; Zeigler, S.; Marocco, S. Classification of plantar pressure and heel acceleration patterns using neural networks. In Proceedings of the 2005 IEEE International Joint Conference on Neural Networks, Montreal, QC, Canada, 31 July–4 August 2005; Volume 5, pp. 3007–3010.
49. Sazonov, E.S.; Fulk, G.; Hill, J.; Schutz, Y.; Browning, R. Monitoring of posture allocations and activities by a shoe-based wearable sensor. *IEEE Trans. Biomed. Eng.* **2011**, *58*, 983–990.
50. Tang, W.; Sazonov, E.S. Highly accurate recognition of human postures and activities through classification with rejection. *IEEE J. Biomed. Health Inform.* **2014**, *18*, 309–315.
51. Fulk, G.D.; Sazonov, E. Using sensors to measure activity in people with stroke. *Top. Stroke Rehabil.* **2011**, *18*, 746–757.
52. Zhang, T.; Fulk, G.D.; Tang, W.; Sazonov, E.S. Using decision trees to measure activities in people with stroke. In Proceedings of the 2013 35th Annual International Conference of the IEEE Engineering in Medicine and Biology Society (EMBC), Osaka, Japan, 3–7 July 2013; pp. 6337–6340.
53. Zhang, T.; Lu, J.; Uswatte, G.; Taub, E.; Sazonov, E.S. Measuring gait symmetry in children with cerebral palsy using the SmartShoe. In Proceedings of the 2014 IEEE Healthcare Innovation Conference (HIC), Seattle, WA, USA, 8–10 October 2014; pp. 48–51.
54. Bae, J.; Kong, K.; Byl, N.; Tomizuka, M. A mobile gait monitoring system for abnormal gait diagnosis and rehabilitation: A pilot study for Parkinson disease patients. *J. Biomech. Eng.* **2011**, *133*, 041005.
55. F-Scan System. Available online: <https://www.tekscan.com/products-solutions/systems/f-scan-system> (accessed on 10 August 2016).

56. Pedar System. Available online: <http://novel.de/novelcontent/pedar> (accessed on 10 August 2016).
57. Lemaire, E.D.; Biswas, A.; Kofman, J. Plantar pressure parameters for dynamic gait stability analysis. In Proceedings of the 28th Annual International Conference of the IEEE Engineering in Medicine and Biology Society, New York, NY, USA, 30 August–3 September 2006; pp. 4465–4468.
58. Catalfamo, P.; Moser, D.; Ghoussayni, S.; Ewins, D. Detection of gait events using an F-Scan in-shoe pressure measurement system. *Gait Posture* **2008**, *28*, 420–426.
59. El Kati, R.; Forrester, S.; Fleming, P. Evaluation of pressure insoles during running. *Procedia Eng.* **2010**, *2*, 3053–3058.
60. FootMoov. Available online: <http://www.footmoov.com> (accessed on 5 August 2016).
61. Tognetti, A.; Lorussi, F.; Carbonaro, N.; de Rossi, D. Wearable Goniometer and Accelerometer Sensory Fusion for Knee Joint Angle Measurement in Daily Life. *Sensors* **2015**, *15*, 28435.
62. Sciavicco, L.; Siciliano, B. *Modelling and Control of Robot Manipulators*; Springer-Verlag: London, UK, 2000.
63. Karantonis, D.M.; Narayanan, M.R.; Mathie, M.; Lovell, N.H.; Celler, B.G. Implementation of a real-time human movement classifier using a triaxial accelerometer for ambulatory monitoring. *IEEE Trans. Inf. Technol. Biomed.* **2006**, *10*, 156–167.
64. Luinge, H.J.; Veltink, P.H. Inclination measurement of human movement using a 3-D accelerometer with autocalibration. *IEEE Trans. Neural Syst. Rehabil. Eng.* **2004**, *12*, 112–121.
65. Sabatini, A.M.; Martelloni, C.; Scapellato, S.; Cavallo, F. Assessment of walking features from foot inertial sensing. *IEEE Trans. Biomed. Eng.* **2005**, *52*, 486–494.
66. BTS SMART-DX. Available online: [www.btsbioengineering.com/products/kinematics/bts-smart-dx](http://www.btsbioengineering.com/products/kinematics/bts-smart-dx) (accessed on 10 August 2016).
67. Truong, P.H.; Lee, J.; Kwon, A.R.; Jeong, G.M. Stride Counting in Human Walking and Walking Distance Estimation Using Insole Sensors. *Sensors* **2016**, *16*, 823.
68. Pappas, I.P.I.; Keller, T.; Mangold, S.; Popovic, M.R.; Dietz, V.; Morari, M. A reliable gyroscope-based gait-phase detection sensor embedded in a shoe insole. *IEEE Sens. J.* **2004**, *4*, 268–274.
69. Winter, D.A. *Biomechanics and Motor Control of Human Gait: Normal, Elderly and Pathological*; University of Waterloo Press: Waterloo, ON, Canada, 1991.



© 2016 by the authors; licensee MDPI, Basel, Switzerland. This article is an open access article distributed under the terms and conditions of the Creative Commons Attribution (CC-BY) license (<http://creativecommons.org/licenses/by/4.0/>).